Phenomenological characterization and thermal analysis of flame spread over jet fuel: influence of radiant exposure time

Manhou Li[1] · **Chao Zhang**[1] · **Lida Sun**[1] · **Shenlin Yang**[1,2] · **Yiran Zhao**[1] · **Huilong Jiang**[1]

Abstract

The high-temperature objects widely exist in industrial and civil building such as the nearby burning pool fires, the heated walls and the hot smoke layer accumulated on ceilings. The output of radiant energy from the adjacent high-temperature objects may accelerate the flame spread. In this paper, a set of well-designed laboratory-scale experiments are carried out to reveal the combustion behavior and flame spread over jet fuel of RP-3 with different radiant heat fluxes and radiant exposure times. Several characteristic parameters, namely flame height, flame spread rate, fuel surface temperature and velocity of subsurface flow, are quantified and analyzed to describe the flame spread behaviors. The average flame height is augmented by the time-integrated radiant heat flux due to the accumulative heat flux and the expanded combustion area. Similarly, measurements of flame spread rate and liquid fuel temperature identify that they are sensitive to the applied radiant flux, but this sensitivity decreases as the flame volume and the blockage effect increase. The external radiant heat flux can simultaneously influence the flame spread from both gas and liquid phases. The thermal exchange and fluid motion involving flame spread under varied external radiant conditions are revealed. The theoretical formula between the fuel surface temperature and the time-integrated radiant heat flux is established based upon the energy conservation law and the thermal boundary layer theory. The current results possess the practical guiding importance for the development of liquid spilling fire disposal measures under the radiations of external heat flux.

Keywords Flame spread · Jet fuel · Radiant exposure time · Thermal exchange

Introduction

It is generally accepted that the heat radiation from the neighboring high-temperature objects, such as the burning pool fires, the heated walls and the hot smoke layer accumulated on ceilings, may increase fire risk and accelerate flame spread. In actual fires, the flame temperature is as high as hundreds of degrees Celsius. The radiant heat flux may ignite the adjacent combustible materials to expand the scope of the uncontrollable combustion. For instance, the jet fuel is widely used for aircraft engine owing to its excellent combustion performance, such as the high calorific value, stable combustion, and low carbon deposition. In case of an accidental ignition of the spilling liquid-phase jet fuel, the strong heat radiation is subsequently caused. Thus, it possesses the practical guiding importance to study the performance of flame spread over jet fuel under the radiations of external heat flux.

The influence of thermal radiation on fire developments including the ignition, flame spread, pool fire, solid pyrolysis and heat transfer has been extensively investigated. The gas-phase spontaneous ignition of horizontal solid materials imposed to external heat flux was numerically investigated by Nakamura [1]. It was concluded that the occurrence of the spontaneous ignition was easily achieved under the external heat flux. Saito [2] and Brehob and Kulkarni [3] independently proposed that the flame spread over solid materials did not maintain in the absence of external heat flux, but did sustain with the assistance of the externally applied radiation source. Similar results were achieved by Osorio et al. [4] who confirmed that the application of radiant flux increased the possibility of the occurrence of flame spread. The flame propagation and flame acceleration were not observed until

✉ Manhou Li
  mhli@hfut.edu.cn

1 School of Civil Engineering, Hefei University of Technology, Hefei 230009, China

2 Anhui International Joint Research Center on Hydrogen Safety, Hefei 230009, China

the heat flux reached a critical value. Femandez-Pello [5] investigated the behaviors of flame spread over polymethyl methacrylate (PMMA) sheets under the externally applied radiation. Measurements of the position of the pyrolysis front were conducted under various heat fluxes in combination with varied radiant exposure times prior to ignition. The fuel surface temperature as well as the flame spread rate increased rapidly once the PMMA was preheated by the radiant flux. Quintiere [6] studied the performances of flame spread over several solid materials under the influence of externally applied heat fluxes. In order to successfully ignite these solids, the radiant exposure time was controlled in the range of 0–300 s. It was discovered that the square root of the flame spread rate increased linearly with the radiant heat flux. Wang et al. [7] endeavored to reveal the influence of external heat flux on flame spread over inclined wood surfaces. The heat feedback from radiant plate to the preheating zone was augmented by the radiant heat flux, while the pyrolysis time was shortened. Chen et al. [8] investigated the effects of external heat flux on combustion behaviors of porous beds soaked with alcoholic fuels. With an increase in radiant intensity, the maximum temperature in the porous bed and the duration time of combustion increased. Farahani et al. [9] confirmed that a convection-driven cavity was formatted during the ice melting process under the exposure of heat flux. The cavity intrusion length was augmented by the heat flux, while the cavity width was attenuated.

The fuel temperature gradually increases in event of an externally applied radiation imposed to the liquids. The initial temperature during liquid spilling is generally lower than the flashpoint of such fuels. The spread of flame in this temperature range belongs to the preheated mode, also called the liquid phase-controlled regime [10]. Accordingly, the heat and mass transfer processes are closely related to the flow field around a flame. The subsurface flow plays a significant role in preheating the bulk of cold liquids ahead of the leading edge of a flame [11]. The explorations of the structure, velocity, temperature profile, and heat flux of subsurface flow were performed by pioneering researchers to understand the controlling mechanisms of flame spread over liquid fuels. Ito et al. [12] calculated the heat transfer through subsurface flow by supposing that the shear force inside the boundary layer was equal to the viscous force. Takahashi et al. [13] performed scaling and instability analyses on the subsurface flow for flame spread over alcoholic fuels. Degroote and Garcia-Ybarra [14] reported that liquid convection was merely built in pulsating regime, but not in the uniform regime.

In total, the influence of the externally applied radiation on solid and liquid fires has been investigated by previous scholars. It was discovered that the ignition sensitivity and fire development speed were augmented once the combustible fuels were exposed to heat flux. The longer radiant exposure time was also expected to increase the fire scale as the total heat absorbed by the fuel (time-integrated radiant heat flux) increased. To date, however, less work is conducted to appreciate the effect of radiant exposure time on flame spread over liquid fuel. Meanwhile, the fluid flow and thermal exchange involving in flame spread with externally applied radiations are very complicated issues which deserve a systemic study. The reinforcement of flame spread rate by externally applied heat radiation depends greatly on the fluid flow and thermal exchange in the gas adjacent to the liquid surface, i.e., the stratification of the fuel vapors, the establishment and destroying of gas-phase recirculation cell and the entrainment of surrounding air. The current investigation puts emphasis on the above-mentioned drawbacks. In order to achieve these objectives, a set of well-designed laboratory-scale experiments are carried out on the combustion and flame spread over jet fuel of RP-3 with different radiant heat fluxes and radiant exposure times.

Experimental

The linear stainless steel tray with the aspect ratio greater than 20 (100 cm long by 4.4 cm wide by 2.5 cm deep) was employed for the tests. The experimental tray was used in our previous studies [15]. The jet fuels were heated or cooled to required temperature using a cooling device or an electric heating plate, and then, they were poured into the experimental tray. The flame spreading was initiated once the desired temperature was achieved. Due to the relative short time for flame spreading, the temperature variation caused by the natural convection was negligible. The flame propagation was initialized at one extreme of the tray using a propane torch. In order to eliminate the heat feedback from the pilot flame to liquids, a small ignition region was isolated by a baffle barrier. When the propane burned out, the baffle barrier was removed to allow the RP-3 flame to proceed freely forward. The flame was extinguished with a fire insulation board as soon as it fully involved within the tray. The flame appearance was monitored by a 25-frame per-second camera; synchronously, the spatial temperatures near liquid surface were recorded by eight 0.5-mm-diameter K-type thermocouples with the responding time of 0.1 s. Four thermocouples are distributed on oil surface with the horizontal distance of 5 cm, while the other four thermocouples are placed 5 mm above oil surface with the same horizontal distance.

As shown in Fig. 1, the various heat fluxes were produced using a 60 cm-long-by-10 cm-wide silicon carbide heating panel combined with an electronic voltage regulator. The high-temperature electric heating wire was used as the heating element to generate the heat flow. The radiant heat was distributed uniformly onto the liquid surface. The radiant
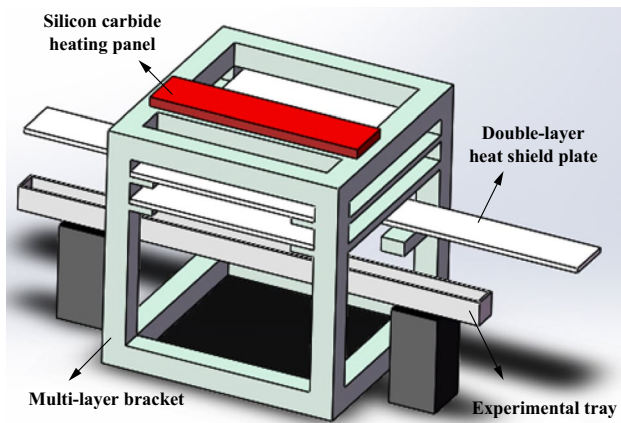
Fig. 1 Scaffolding platform for heating panel

intensity declined significantly as the interval distance between the radiant panel and the fuel surface increased. The fully developed diffusion flame had a limited height approximately 10 cm. Thus, the heating panel was placed 20 cm above the fuel surface to minimize interference with the flow induced by the fire and synchronously produce measurable effects on the flame spread rate [16].

The infrared electric heating panel was fixed in the top of the multilayer scaffolding platform. The oil tray was placed at the bottom of the platform. The 3-cm-thick double-layer heat shield board was arranged longitudinally between the heating panel and the flame spread tray. Before the electric heating panel reached the stable radiant intensity, the pre-heating energy from the electric heating panel to the fuel surface was completely inhabited. After the electric heating panel attained the steady radiation, the heat shield board was removed. The whole flame spreading process was exposed to the externally applied radiant heat flux. The *radiant exposure time* was defined as the time that the oil surface was roasted by the heating panel before the flame spreading was initiated. The radiant exposure time was easily controlled because the heat radiation was terminated immediately once the heat shield board was inserted again. The detailed experimental arrangements are demonstrated in Table 1. In order to eliminate the experimental uncertainties, each data point reported in this paper is an average value from three tests.

Table 1 Experimental arrangement

Experimental tray size (length × width × depth, cm³)	100 × 4.4 × 2.5
Fuel type	Jet fuel of RP-3
Flashpoint/°C	46
Radiant exposure time, τ/s	0, 20, 40, 60, 80, 100, 120, 140
Radiant intensity, $\dot{q}_{er}$/kW m^{-2}	0, 1.1, 1.69, 2.25, 2.8, 3.6
Initial fuel temperature/°C	25, 40

In the current research, the magnitude of desired radiant intensity was achieved by calibrating the electronic voltage regulator. The output of radiant energy was specified by the MR-5-type radiant heat sensor. As displayed in Table 2, six radiant intensities, namely 0, 1.1, 1.69, 2.25, 2.8 and 3.6 kW m^{-2}, were applied in this study. The corresponding temperatures on the surface of radiant panel were 25, 330, 415, 475, 530 and 580 °C. The radiant exposure time (τ) was changed in the range of 0–140 s, with the interval time of 20 s.

According to the Stefan–Boltzmann law, the radiant heat flux from the infrared plate is correlated as follows [17]:

$$\dot{q}_{er} = \varepsilon \cdot \sigma \cdot T_s^4 \tag{1}$$

where $\dot{q}_{er}$ is the radiant output from the radiant panel, ε is the emissivity of the radiant panel, for black-body radiation, $\varepsilon = 1$, σ is the Stefan–Boltzmann constant and T_s is the surface temperature of the radiant panel. According to the inverse-square law [18], the radiant heat flux decreases with the squared distance because the radiant area increases by square of distance. The surface emissivity of the radiant panel is estimated by the ratio of measured and calculated values of the radiant heat flux with the distance of 20 cm. Figure 2 shows that the average value of the surface emissivity of the radiant panel is about 0.52.

Results and discussion

Flame appearance and oscillation

Figure 3 shows the typical flame appearances under varied heat fluxes and radiant exposure times. When the flammable liquid is subjected to the externally applied radiation, according to the principle of transient heat transfer, the temperature of the liquid rises with time. Under continuous heating, the liquid evaporates and the combustible gas escapes from the liquid surface to mix with oxygen [19]. Once the lean flammability limit of the fuel vapor is attained, the flame spreads quickly forward.

The flame configuration possesses a serrated and corrugated shape during the flame propagation [20]. This is owing to the inhomogeneous distribution of the fuel vapors above oil surface. In the leading portion of the flame contour, the flame attaches to the liquid surface with

Table 2 Radiant intensities and temperatures of radiant plate at various input voltages

Input voltage/V	120	140	160	180	200
Radiant intensity/kW m^{-2}	1.1	1.69	2.25	2.8	3.6
Temperature of radiant panel/°C	330	415	475	530	580

Fig. 2 Correlation of radiant heat flux with temperature of radiant panel surface
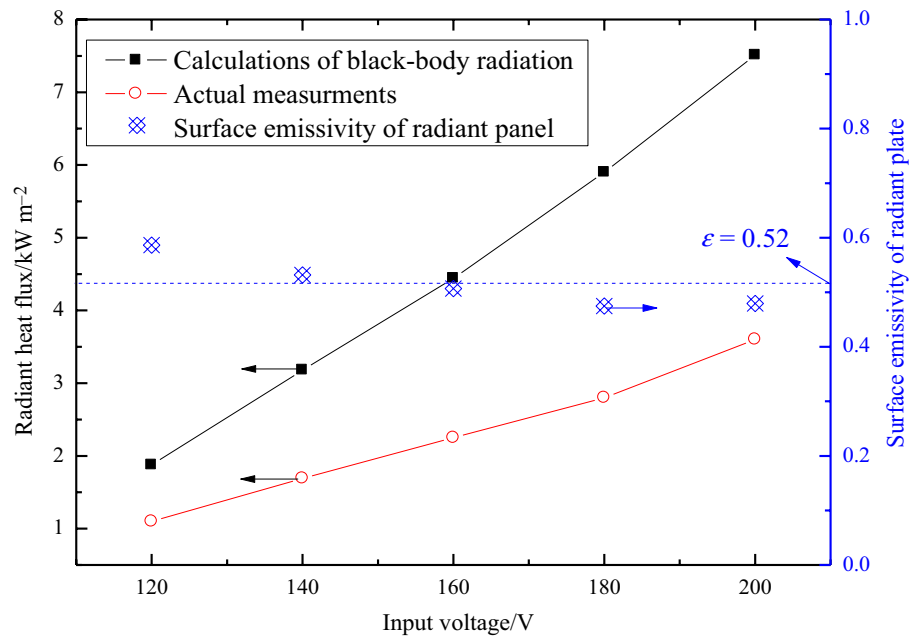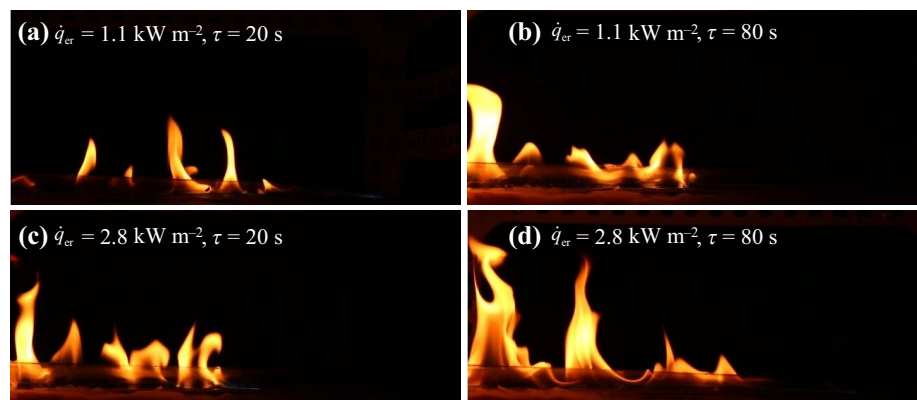

Fig. 3 Sample flame appearances for flame spread under varied externally applied radiations

a low flame height. By contrast, in the trailing portion of the flame, the flame height is relative high. The flame height shows a fluctuating variation versus time at each radiation condition. This oscillation is mainly due to the boundary layer instability between the fire plume and the surrounding air. This instability is positively related to the buoyancy-induced lift by the flame counter [21].

The transient flame heights in the trailing portion of the flame are shown in Fig. 4. The average flame heights are also displayed in this figure with several point segment lines. The average flame height at $\dot{q}_{er} = 1.1\,\mathrm{kW\,m^{-2}}$, $\tau = 80$ s is almost equal to that at $\dot{q}_{er} = 2.8\,\mathrm{kW\,m^{-2}}$, $\tau = 20$ s, thus the average values of flame heights in both cases are drawn by point segment line with red color. The flame height increases with the radiant exposure time or radiant intensity. This is due to the accumulative heat

flux which preheats the surrounding air temperature and expands the combustion area, making an augmentation of the convective entrainment of the fire plume [22].

For pool fire with a large aspect ratio (the ratio of length to width is larger than 3), the flame height is predicted by the following correlation [23]:
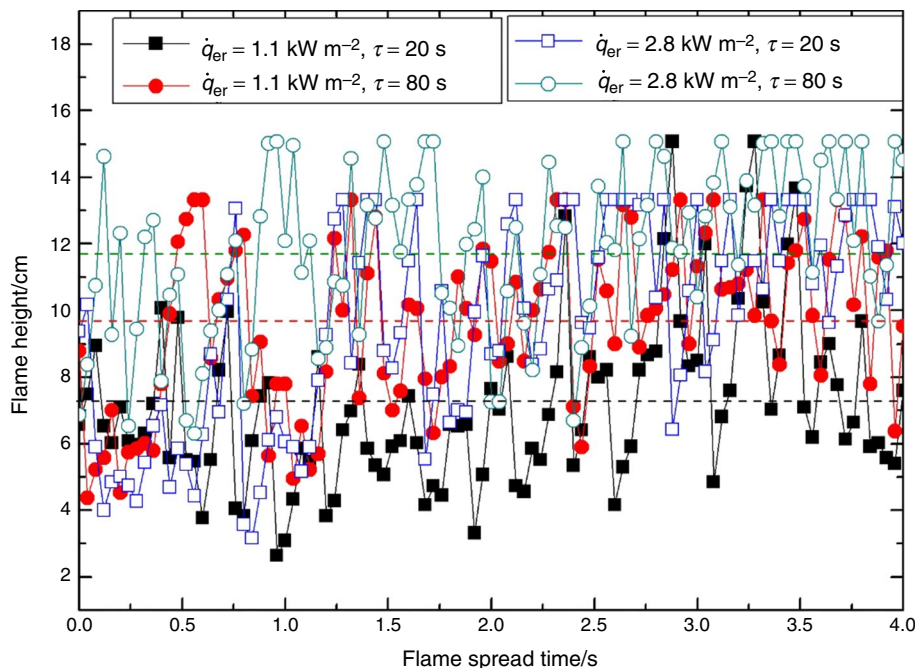
$$H = 0.035(\dot{q}_0/L)^{2/3} \tag{2}$$

where L is the length of the tray and $\dot{q}_0$ is the heat release rate.

$$\dot{q}_0 = \dot{m}'' \cdot A \cdot \eta \cdot h_c \tag{3}$$

where $\dot{m}''$ is the burning rate, A is the area of the burning tray, η is the constant and h_c is the heat of combustion for the complete combustion of liquid fuel. Then, Eq. (3) yields,

$$H = 0.035(\dot{m}'' \cdot W \cdot \eta \cdot h_c)^{2/3}. \tag{4}$$

The time-integrated radiant flux is augmented by the longer radiant exposure time or the larger radiant intensity, producing the larger burning rate $\dot{m}''$. The flame diffuses further off the burning pool surface to enlarge the flame height which in turn enhances the temperature around flame and entrainment velocity along the axis of the turbulent flame plume. The convective heat transfer and flame radiation are promoted to induce the large amount of radiant heat feedback from the flame counter to liquid surface [4]. Consequently, the heat accumulation into the flame structure accelerates the flame spread rate.

Thermal exchange of flame spread under externally applied radiation

The schematic diagram of flame spread over liquid fuel under the externally applied heat flux is shown in Fig. 5. The externally applied heat flux distributes uniformly onto the liquid surface. Meanwhile, the cold liquids receive energy from the flame radiation, the gas-phase and liquid-phase heat conduction. More importantly, during the flame propagation, the hot fluids move forward through the subsurface flow. The subsurface flow, also named as the thermo-capillary flow, is driven by combined effects of surface tension and buoyant force. The subsurface flow preheats the cold fuels in the manner of liquid-phase heat convection [24].

The influence of externally applied radiation appears in both downstream and upstream regions of the flame. On the one hand, increasing the radiant exposure time and radiant

Fig. 5 Schematic illustration of flame spread over liquid fuel under externally applied radiation
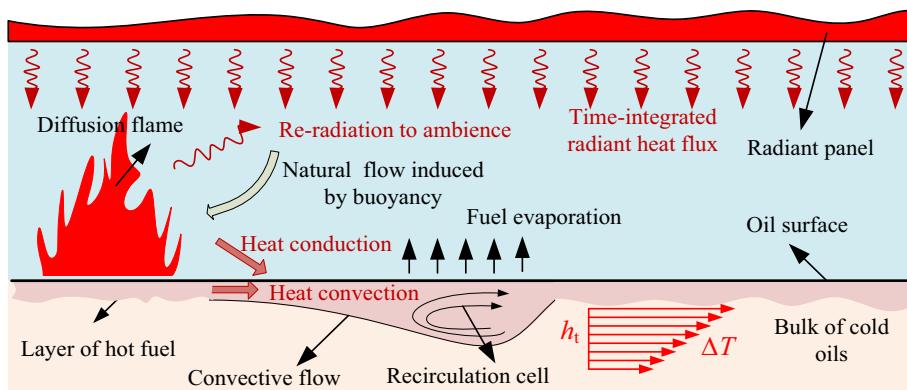
flux upraises the fuel surface temperature and fuel vapor concentration in the downstream region of the flame counter, which further enhances the flame volume and consequently an expanding of the spatial distribution of the flame structure [25]. On the other hand, the exposure of cold fuels to the thermal radiation increases the liquid temperature prior to flame tip arrival. The additional energy provided by the externally applied heat flux warms the subsurface flow region. Both factors are complicated phenomena which contain the heat absorption and dissipation in the gas and liquid phases, the reflection and re-radiation at the gas–liquid phase interface and the liquid-phase convective cooling by boundary layer generated by the radiation-heated surface [26].

Temperature evolution and flame spread rate

The fuel temperature is an imperative parameter in analyzing the behaviors of flame spread. Under $\dot{q}_{er} = 1.1$ kW m^{-2} and $\tau = 20$ s, the temperature distributions in both liquid and gas phases are displayed in Fig. 6. During the radiant exposure time of 20 s, the fuel surface temperature increases from 25 to 28.5 °C. At the moment of t_2, the fuel surface temperature increases evidently because the front of the subsurface flow arrives the measuring point of the thermocouple. Then, a dramatic increase in the gas-phase temperature occurs at t_3 in which the flame's leading edge arrives.

The flame spread rate is the time-dependent quantity because of the intrinsic pulsation of flame spreading. Thus, all measurements of the flame spread rates are the average values which are calculated by a certain flame

propagation distance, ~30 cm. For a given radiant intensity of 2.8 kW m^{-2}, Fig. 7 shows the flame spread rate and fuel surface temperature versus radiant exposure time at $T_0 = 25$ and 40 °C, respectively. Figure 8 systematically illustrates the fuel surface temperature versus radiant exposure time at various radiant intensities. The results prove that the temperature increases violently initially but ascends slowly after a period of radiant exposure time. This means that after the fuel surface temperature approaches a certain threshold, the time-integrated radiant flux is principally used for evaporating the liquid rather elevating the liquid's temperature.

There are multiple reasons to account for these phenomena. First, the liquid fuels are cooled by the opposed gas movement induced by natural flow. Second, the huge heat sink by the liquid fuel in the tray restricts the liquid temperature to a certain threshold [9]. Third, the radiant heat feedback from the flame is negligible for the small flamelet in the leading edge of the flame. However, in the trailing portion of the flame, the flame volume is considerably enhanced by the externally applied heat flux, as displayed in Fig. 3. Accordingly, the heat flux imposed by the externally applied radiation becomes less and less significant in comparison with the fire feedback [27]. Eventually, the re-radiation heat loss from the liquid surface is augmented as the fuel surface temperature.

In the initial stage of the utilization of the external radiation, the additive heat flux is mainly used for elevating the liquid temperature, other than for evaporating the liquid fuels. The total energy absorbed by the liquid surface Q_t is estimated on the basis of the energy conservation law,

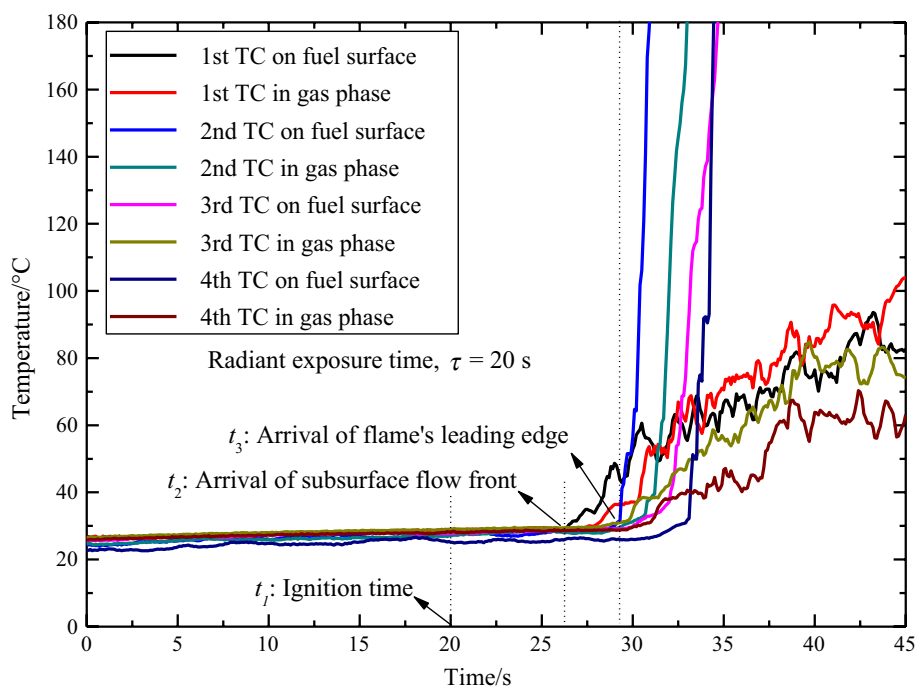**Fig. 6** Temperature distribution in both liquid and gas phases

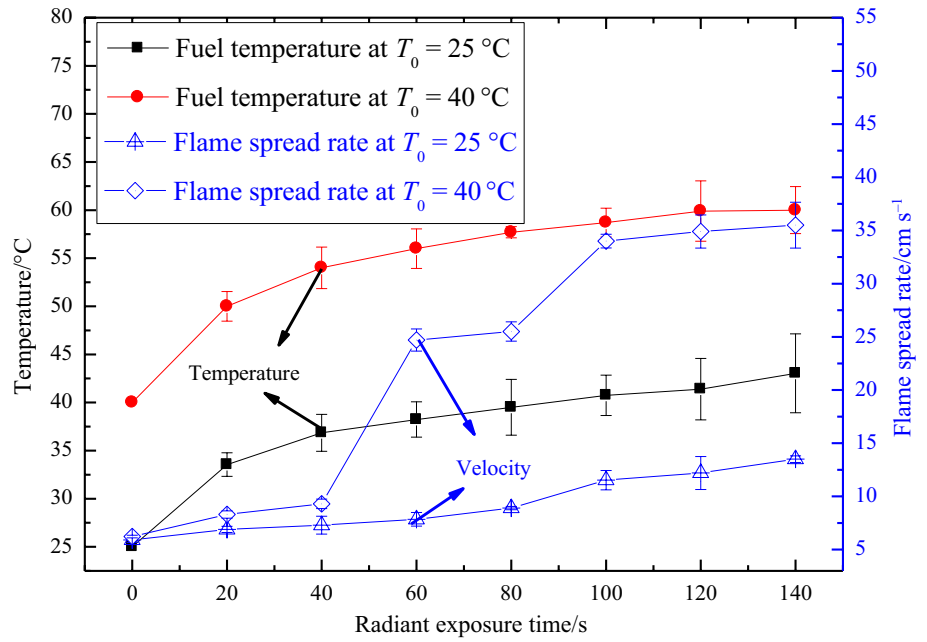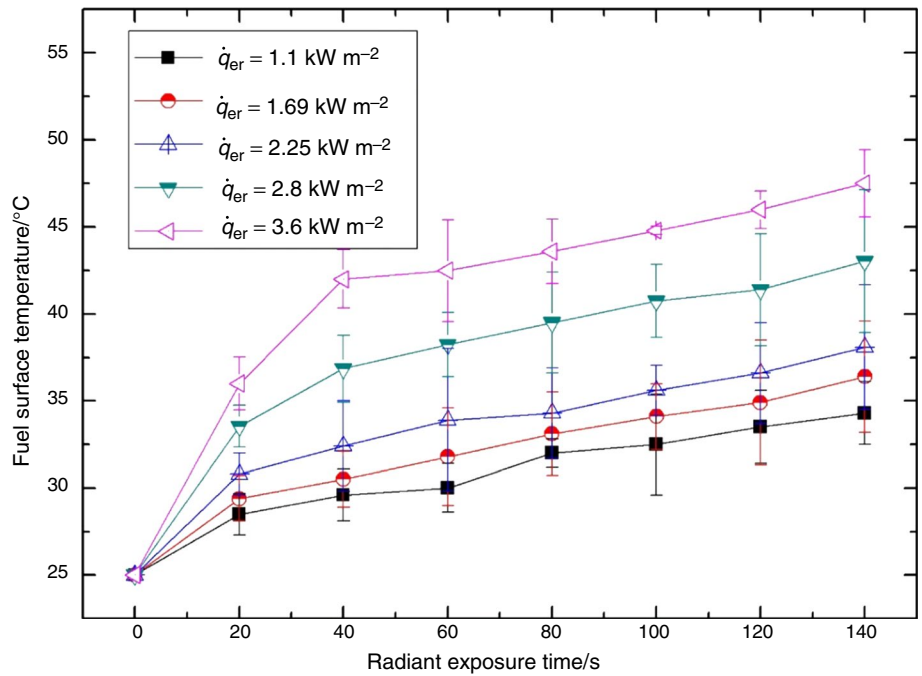**Fig. 7** Flame spread rate and fuel surface temperature versus radiant exposure time

Fig. 8 Fuel surface temperature versus radiant exposure time at various radiant intensities

$$Q_t = \dot{q}_{er} \cdot A \cdot \tau = m \cdot c_p \cdot \Delta T \tag{5}$$

where m is the local mass of the liquid fuel, c_p is the specific heat capacity of RP-3, approximately 2.05 kJ kg^{-1} °C^{-1}, and ΔT is the average temperature difference within the vertical thermal boundary layer. Two assumptions are made inside the vertical thermal boundary layer. First, the vertical temperature distributes linearly inside the boundary layer, as shown in Fig. 5. Second, the imposed heat flux is transferred to the liquids inside the boundary layer solely through the

heat conduction. Then, the temperature difference is calculated by the time-integrated radiant heat flux,

$$\Delta T = 2 \cdot \frac{\dot{q}_{er} \cdot \tau}{\rho \cdot c_p \cdot h_t} \tag{6}$$

where ρ is the liquid density and h_t is the thermal boundary layer thickness which is experimentally measured by Guo et al. [28] using a Schlieren photography technique. It is

Fig. 9 Comparison of predicted and measured values of temperature difference in fuel surface and cold oils
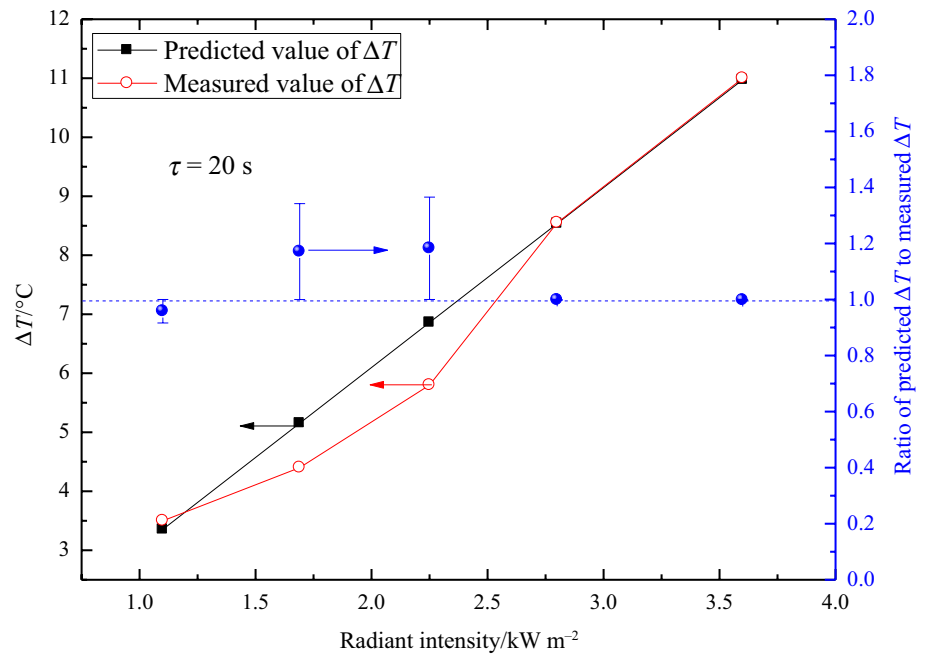
confirmed that the value of h_t is approximately 8 mm for jet fuel, regardless of initial fuel temperature.

For a given radiant exposure time $\tau = 20$ s, Fig. 9 displays the temperature differences between the fuel surface and bulk of cold oils. Apparently, the measurements of temperature difference are acceptably consistent with the predicting model.

Figure 10 shows flame spread rate versus radiant exposure time and radiant intensity. Under $\dot{q}_{er} = 3.6$ kW m^{-2}, the flame

spread rate increases violently as the radiant exposure time increases. In such cases, the fuel vapor concentration has already exceeded the lean flammability limit; thus, the flame spreads in the manner of premixed combustion, without any preheating of liquid flow.

For $\dot{q}_{er} < 3.6$ kW m^{-2}, the measurements of flame spread rate identify that they are sensitive to the radiant flux, but this sensitivity decreases as the flame volume and the blockage effect increase. The high-temperature pool surface

Fig. 10 Flame spread rate versus radiant exposure time at various radiant intensities
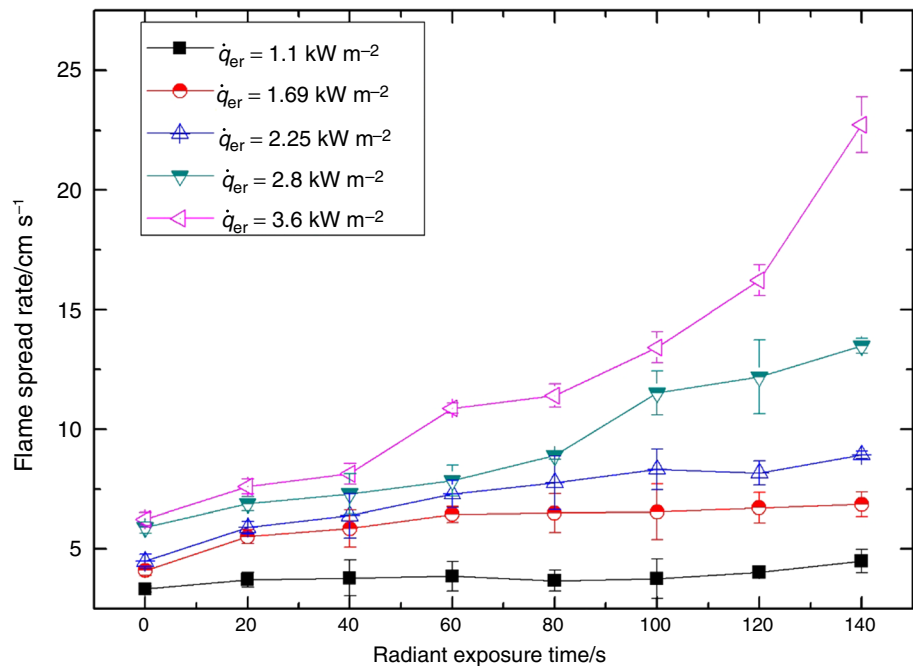
augments the amount of the re-radiation energy of liquid surface and subsequently attenuates the radiation influence on flame spread rate. As the liquids are subjected to the increased radiant exposure time, more and more combustible vapors are accumulated above the liquid surface. The liquid fuels and the fuel vapors serve as the strong heat sink because the great amount of heat is absorbed in the mid-infrared and near-infrared band [29]. The absorbed heat flux during the passage of the thermal radiation through the flammable vapor layer is augmented. Meanwhile, the gas products and the soot produced by the fuel combustion hinder the radiant heat flux imposed to fuel surface [25]. Consequently, the external radiant energy actually received by the cold oil is significantly smaller than the ideal value. The results are in accordance with the previous observations reported by Shih [30].

Under the condition of $T_0 = 25$ °C and $\dot{q}_{er} = 1.1$ kW m^{-2}, the fuel surface temperature is measured at different radiant exposure times. The fuel surface temperature arrives at 28.4, 30.2, 31.5, 32.6, 33.4, 34.2 and 34.9 °C for the radiant exposure time of 20, 40, 60, 80, 100, 120 and 140 s, respectively. The flame spread rates at different radiant exposure times are plotted in Fig. 11. Simultaneously, the non-radiant flame spread rates with initial temperatures equal to the corresponding temperatures are presented in this figure.

Figure 11 indicates that the flame spread rates without externally applied radiation are significantly smaller than those with radiations. In the absence of external radiation, the liquid temperature is higher than that of the surrounding

cold air. As the flame front approaches, a great amount of energy is absorbed by the liquid fuels. The heat loss from flame configuration to cold air is disadvantage for the flame propagation [31]. In the case of externally applied radiation, on the contrary, the air around the flame has already been warmed before the flame approaches. The hot air accelerates the fuel evaporation rate and thereby increases the flame spread rate. This phenomenon fully demonstrates that the external radiant heat flux can simultaneously influence the flame spread through both gas and liquid phases.

Scale and velocity of subsurface flow

The subsurface flow merely appears in liquid phase-controlled flame spread regime with the maximum value of the movement velocity ~ 10 cm s^{-1}. Otherwise, the gas-phase-controlled flame spread is attained and the convective flow disappears. Figure 12 shows that as the radiant exposure time increases, the increasing rate of subsurface flow velocity tends to diminish. This coincides with the measured liquid surface temperature: The sensitivity of the fuel surface temperature is less marked as the radiant exposure time increases [32].

The velocity of subsurface flow possesses the same order of magnitude as the flame spread rate. The velocity of subsurface flow is estimated based on the hypothesis that the shear force is equal to the surface tension in the boundary layer [11],

Fig. 11 Comparison of flame spread rate with and without externally applied radiation
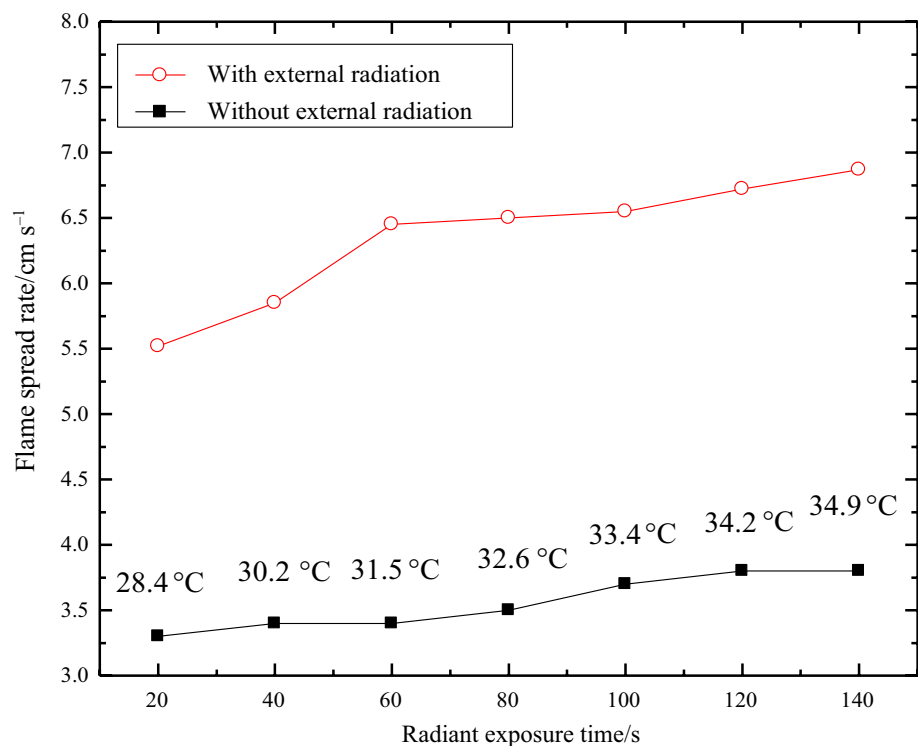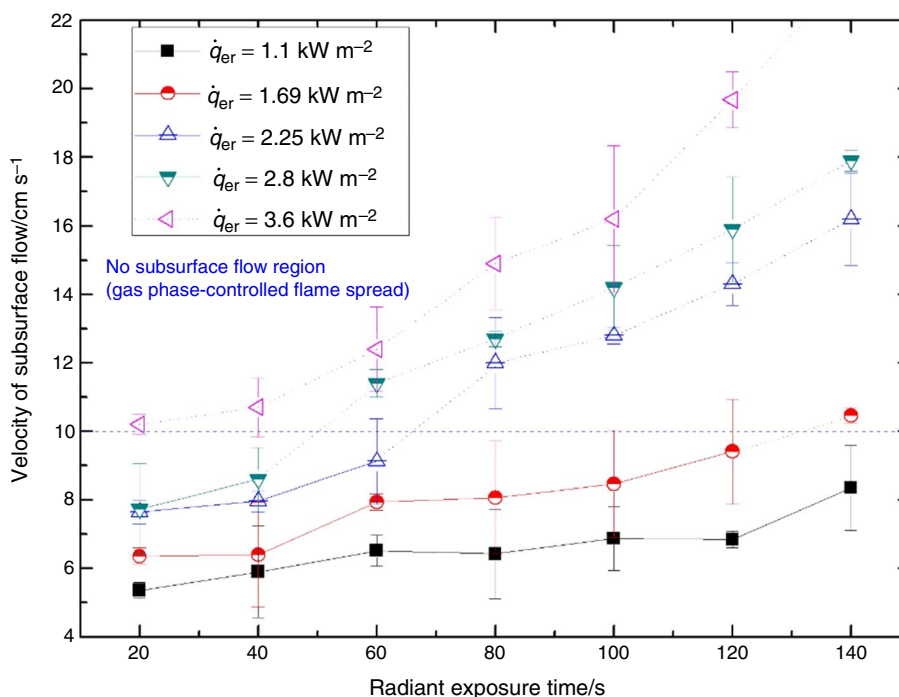
Fig. 12 Velocity of subsurface flow versus radiant exposure time at various radiant intensities

$$u_s = \sigma_T h_*(T_F - T_0)/(\mu L_*) \tag{7}$$

where T_F is the fuel temperature beneath the flame, μ is the dynamic viscosity, σ_T is the surface tension coefficient with temperature and h_* is the characteristic depth of subsurface flow.

As the radiant exposure time increases, the temperature difference ΔT between the hot fuels beneath flame shape and the bulk of cold oils increases. Meanwhile, the dynamic viscosity μ decreases as the liquid temperature increases. Both factors induce the faster subsurface flow velocity and the larger flame spread rate [26].

Conclusions

The phenomena and thermal analysis of flame spread over jet fuel of RP-3 are characterized, and the influence of radiant exposure time on flame spread is discussed. Main conclusions are summarized as follows:

1. The average flame height is augmented by the time-integrated radiant heat flux due to the accumulative heat flux and the expanded combustion area.
2. Measurements of flame spread rate and liquid fuel temperature identify that they are sensitive to the applied radiant flux, but this sensitivity decreases as the flame volume and the blockage effect increase.
3. The measurements of temperature difference are acceptably consistent with the predicting model.

4. The externally applied radiation simultaneously influences the flame spread over liquid fuel through gas and liquid flows.

References

1. Nakamura Y, Yamashita H, Takeno T, Kushida G. Effects of gravity and ambient oxygen on a gas-phase ignition over a heated solid fuel. Combust Flame. 2000;120(1):34–48. https://doi.org/10.1016/S0010-2180(99)00077-2.
2. Saito K, Williams FA, Wichman IS, Quintiere JG. Upward turbulent flame spread on wood under external radiation. J Heat Transf. 1989;111(2):438–45. https://doi.org/10.1115/1.3250696.
3. Brehob EG, Kulkarni AK. Experimental measurements of upward flame spread on a vertical wall with external radiation. Fire Saf J. 1998;31(3):181–200. https://doi.org/10.1016/S0379-7112(98)00012-5.
4. Osorio A, Pello AF, Urban D, Ruff G, editors. External radiant flux and oxygen concentration as conditions for concurrent flame spread in fabrics. In: International conference on environmental systems; 2013 July 15–19, 2012; San Diego, California.
5. Fernandez-Pello AC. Upward laminar flame spread under the influence of externally applied thermal radiation. Combust Sci Technol. 1977;17(3–4):87–98. https://doi.org/10.1080/00102207708946818.
6. Quintiere J. A simplified theory for generalizing results from a radiant panel rate of flame spread apparatus. Fire Mater. 1981;5(2):52–60. https://doi.org/10.1002/fam.810050204.

7. Wang Q, Xiao H, Wan W, Cui Z, Zhu H, Sun J. Flame spread on inclined wood surfaces: influence of external heat flux and ambient oxygen concentration. Combust Sci Technol. 2018;190(1):97–113. https://doi.org/10.1080/00102202.2017.1376665.

8. Chen X, Kong W, Wang B. Effect of external heat flux on combustion behaviors of porous beds soaked with liquid fuels. J Eng Thermophys. 2007;28(5):871–4. https://doi.org/10.3321/j.issn:0253-231X.2007.05.047.

9. Farahani HF, Fu Y, Jomaas G, Rangwala AS. Convection-driven cavity formation in ice adjacent to externally heated flammable and non-flammable liquids. Cold Reg Sci Technol. 2018;154:54–62. https://doi.org/10.1016/j.coldregions.2018.06.010.

10. Degroote E. Control parameters of flame spreading in a fuel container. J Therm Anal Calorim. 2007;87(1):149–51. https://doi.org/10.1007/s10973-006-7838-1.

11. Williams FA. Mechanisms of fire spread. Proc Combust Inst. 1977;16(1):1281–94. https://doi.org/10.1016/s0082-0784(77)80415-3.

12. Ito A, Masuda D, Saito K. A study of flame spread over alcohols using holographic interferometry. Combust Flame. 1991;83(3–4):375–89. https://doi.org/10.1016/0010-2180(91)90084-o.

13. Takahashi K, Ito A, Kudo Y, Konishi T, Saito K. Scaling analysis on pulsating flame spread over liquids. Int J Chem Eng. 2008; Article ID 178292:1–10. https://doi.org/10.1155/2008/178292.

14. Degroote E, Garcia-Ybarra PL. Flame spreading over liquid ethanol. Eur Phys J B. 2000;13(2):381–6. https://doi.org/10.1007/s100510050045.

15. Li M, Fukumoto K, Wang C, Zhang X, Yang S, Liu X. Phenomenological characterization and investigation of the mechanism of flame spread over butanol-diesel blended fuel. Fuel. 2018;233:21–8. https://doi.org/10.1016/j.fuel.2018.06.033.

16. Zhang XL, Vantelon JP, Joulain P. Thermal radiation from a small-scale pool fire: influence of externally applied radiation. Combust Flame. 1993;92(1):71–84. https://doi.org/10.1016/0010-2180(93)90199-d.

17. Hurley MJ, Gottuk D, Hall JR Jr, Harada K, Kuligowski E, Milosh Puchovsky PE, et al. SFPE handbook of fire protection engineering. 5th ed. Berlin: Springer; 2016.

18. Adityo R, Agung R, Satrio P, Nugroho YS. Measurement of thermal radiative heat transfer using a multi-axis heat flux sensor. In: 2nd international Tropical Renewable Energy Conference (I-TREC); 2018/01: IOP Publishing; 2018. p. 012106.

19. Chen X, Lu S, Ding Z. Initial fuel depth effect on the burning characteristics of thin-layer pool fire in a confined enclosure. J Therm Anal Calorim. 2019. https://doi.org/10.1007/s10973-019-08493-1.

20. An W, Sun J, Zhu G. Experimental study on temperature field of upward flame spread over discrete polystyrene foam. J Therm Anal Calorim. 2018;131(3):2647–56. https://doi.org/10.1007/s10973-017-6728-z.

21. Fang J, Tu R, Guan J, Wang J, Zhang Y. Influence of low air pressure on combustion characteristics and flame pulsation frequency of pool fires. Fuel. 2011;90(8):2760–6. https://doi.org/10.1016/j.fuel.2011.03.035.

22. Tang F, He Q, Wen J. Effects of crosswind and burner aspect ratio on flame characteristics and flame base drag length of diffusion flames. Combust Flame. 2019;200:265–75. https://doi.org/10.1016/j.combustflame.2018.11.011.

23. Hasemi Y, Nishihata M. Fuel shape effect on the deterministic properties of turbulent diffusion flames. In: Fire Safety Science International Association for Fire Safety Science; 1988. p. 275–84.

24. Ross HD. Ignition of and flame spread over laboratory-scale pools of pure liquid fuels. Prog Energ Combust. 1994;20(1):17–63. https://doi.org/10.1016/0360-1285(94)90005-1.

25. Zhang XL, Vantelon JP, Joulain P, Fernandez-Pello AC. Influence of an external radiant flux on a 15-cm-diameter kerosene pool fire. Combust Flame. 1991;86(3):237–48. https://doi.org/10.1016/0010-2180(91)90104-J.

26. Kashiwagi T. A study of flame spread over a porous material under external radiation fluxes. Symp Int Combust. 1975;15(1):255–65. https://doi.org/10.1016/S0082-0784(75)80302-X.

27. Chen M, Dongxu O, Cao S, Liu J, Wang Z, Wang J. Effects of heat treatment and SOC on fire behaviors of lithium-ion batteries pack. J Therm Anal Calorim. 2019;136(6):2429–37. https://doi.org/10.1007/s10973-018-7864-9.

28. Guo J, Lu S, Wang C. Study on the subsurface flow induced by flame spread over aviation kerosene. J Therm Anal Calorim. 2014;116(1):455–60. https://doi.org/10.1007/s10973-013-3547-8.

29. Zhou Y, Yang L, Dai J, Wang Y, Deng Z. Radiation attenuation characteristics of pyrolysis volatiles of solid fuels and their effect for radiant ignition model. Combust Flame. 2010;157(1):167–75. https://doi.org/10.1016/j.combustflame.2009.06.020.

30. Shih TM. Fire characteristics under the influence of external radiation. In: Joint ASME/AIChE 28th National Heat Transfer Conference; August 6–8, 1979; San Diego, CA.

31. Hirano T, Sato K. Effects of radiation and convection on gas velocity and temperature profiles of flames spreading over paper. Symp Int Combust. 1975;15(1):233–41. https://doi.org/10.1016/S0082-0784(75)80300-6.

32. Zhang XL, Vantelon JP, editors. Radiative transfer at the surface of a small scale pool fire under the influence of external radiation. Heat transfer in radiating and combusting systems. Berlin: Springer; 1991.